X-Ray Ct Analysis of FNS Mortars Mixed with Converter Slag Fine Aggregate

By Won Jung Cho & Ji Seok Kim

Hanyang University

Introduction- Aggregate is an indispensable component in concrete occupying nearly 65-80% of the total volume, whose effects on concrete performance are rarely studied [1]. Due to their inert and impervious characteristics, the durability of concrete is also influenced by the quality of aggregates. To meet the global demand for concrete in the future, it is becoming a more challenging task to find suitable alternatives to natural aggregate for preparing concrete [2]. Hence, the use of alternative sources for natural aggregates is becoming increasingly important.

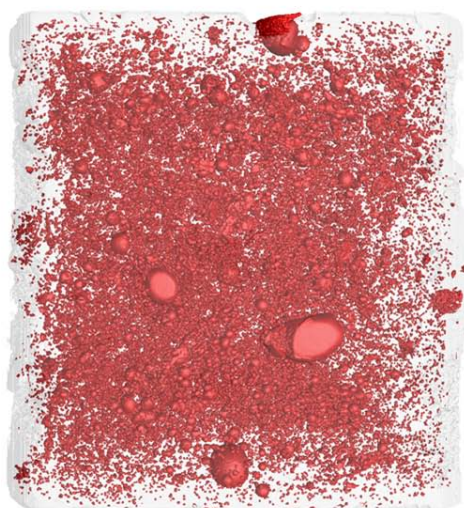XRAYCTANALYSISOFFNSMORTARSMIXEDWITHCONVERTERSLAGFINEAGGREGATE

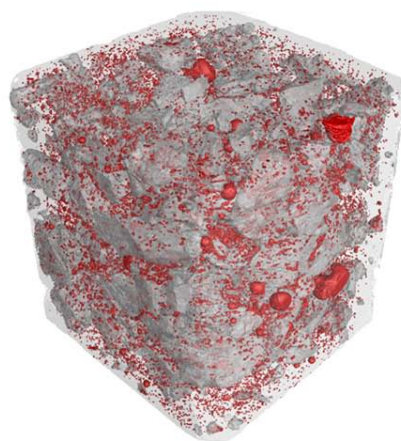*Strictly as per the compliance and regulations of:*

X-Ray Ct Analysis of FNS Mortars Mixed with Converter Slag Fine Aggregate

Won Jung Cho [α] & Ji Seok Kim [σ]


Graphical Abstract-

2-dimensional cross section

3D image

I. Introduction

Aggregate is an indispensable component in concrete occupying nearly 65-80% of the total volume, whose effects on concrete performance are rarely studied [1]. Due to their inert and impervious characteristics, the durability of concrete is also influenced by the quality of aggregates. To meet the global demand for concrete in the future, it is becoming a more challenging task to find suitable alternatives to natural aggregate for preparing concrete [2]. Hence, the use of alternative sources for natural aggregates is becoming increasingly important.

Steel slag is a vast majority of solid wastes produced as a by-product during the steelmaking process. It is reported that 2-4 tons of wastes are being generated per one ton of steel production [3]. In currently, the annual emission of steel slag in China is 101 million tons [4] while 43.43 million tons in Korea but its utilization is very low due to the soundness effect; 1) poor grindability, 2) lower reactivity, 3) bad stability of

volume [5]. Especially, converter slag (BOF) has been suggested a high potential of causing expansion as suggested in Eq (1) when utilized with ordinary Portland cement (OPC), hence its usability as a construction material is very low. Accordingly, the produced BOF is buried or stacked, however, the problems such as storage yard with a width that can be stacked and environmental pollution by leachate generated during the storage process have generated.

$$Free\ CaO + H_2O = Ca(OH)_2 \cdots Eq \qquad (1)$$
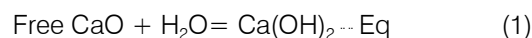
Ferronickel slag (FNS) is an industrial by-product obtained by melting nickel ore and bituminous coal at high temperatures (between 1500℃ and 1600℃) and thereafter separating from ferronickel [6,7]. The main clinker of FNS is Forsterite (Mg_2SiO_4), and it also contains Fe_2O_3, CaO, and Al_2O_3 as an oxide composition. The production of FNS is estimated at about 2 million tons in Korea [6], 30 million tons in China [8] and approximately 3 million tons in Japan annually [9]. For decades, there was an effort to use FNS as a construction material. Due to the depletion of natural aggregate, the use of FNS as a replacement of aggregates has been extensively conducted [7,9-12]. Recently, as the reactivity of FNS was confirmed, the utilization of FNS as a binder was also investigated [8,10]. When mixed with ordinary Portland cement

Author α σ: Department of Civil and Environmental Engineering, Hanyang University, Ansan 15588, Republic of Korea.
e-mail: nelly91@hanyang.ac.kr

(OPC), FNS clinker reacts with $Ca(OH)_2$ to create secondary C-S-H gel, thereby contributing to the long-term strength development [13]. However, it has been still discussed whether FNS can provide a similar performance compared to conventional binders. Huang et al. [8] reported a reduction of compressive strength and chloride penetration resistance of FNS concrete than conventional OPC concrete. On the other hand, some studies showed that the compressive strength of FNS incorporated mortars was similar to the pulverized fly ash (PFA) [6,14]. Recently, economical or environmental advantages have been also reported through comparative analysis with conventional cementitious materials.

The purpose of this study is to investigate the pore structure of mortar which is mixed with FNS binder and fine aggregate replaced by using BOF. In order to characterize the expansion behavior, the pore structure analysis was examined by using X-ray CT analysis.

II. EXPERIMENT WORK

a) Raw materials

i. The particle size distribution of OPC and FNS

The materials used in this study were OPC and electric arc furnace FNS powder produced by Korean company "P." The particle size distribution is shown in Figure 1 (modified from [15].
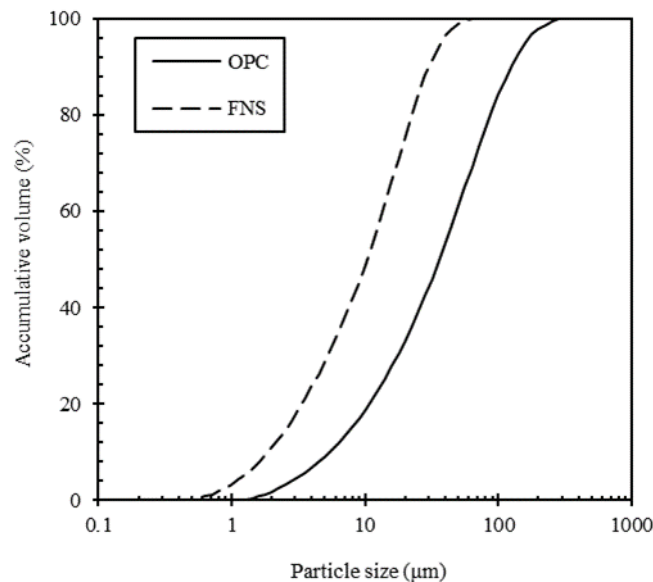

Fig. 1: The particle size distribution of OPC and FNS

ii. X-ray fluorescence (XRF)

Chemical analysis was carried out with X-ray fluorescence (XRF) and shown in Table 1 together with physical properties. The main chemical components of the FNS powders are SiO2, MgO, and Fe2O3. The CaO contents of FNS were counted for only 6.28% which is lower than OPC [15]. BOF fine aggregate has mainly consisted of CaO, SiO2 and Fe2O3, thus BOF can be classified as high calcium and ferrous materials.

Table 1: Chemical and physical properties of raw materials

|	Oxides (%)							Physics		Loss on ignition (%)
	CaO	SiO$_2$	Al$_2$O$_3$	MgO	Fe$_2$O$_3$	SO$_3$	TiO$_2$	Density (g/cm^3)	Fineness (cm^2/g)	
OPC	66.98	17.43	3.97	1.60	4.16	3.41	0.27	3.14	3.539	0.40
FNS	6.28	48.23	3.59	23.01	15.76	0.50	0.11	3.14	3.400	0.02
BOF	44.95	11.60	6.50	2.19	28.12	0.18	-	3.27	-	-

iii. X-ray diffraction (XRD)

Figure 2 presented the X-ray diffraction (XRD) curves of the OPC, FNS and BOF, respectively. In the case of OPC, alite (C3S, 3CaOSiO2) and belite (C2S, 2CaO·SiO2) are the main clinkers while other clinkers such as gypsum, periclase, brownmillerite (4CaO·Al2O3·Fe2O3) accounted for lower quantities. For FNS, the composition mainly accounted for forsterite (Mg2SiO4) and fayalite (Fe2SiO4) which have crystalline nature. Most of the MgO peaks detected from XRF

analysis indicated forsterite and it originally shows very late hydration which takes about 2 years for the complete reaction [16].The BOF sand is also mainly composed of crystalline clinker such as wuestite (FeO), srebrodolskite (Ca2(Fe+3)2O5, mayenite (Ca12Al14O33), and larnite (Ca2SiO4).
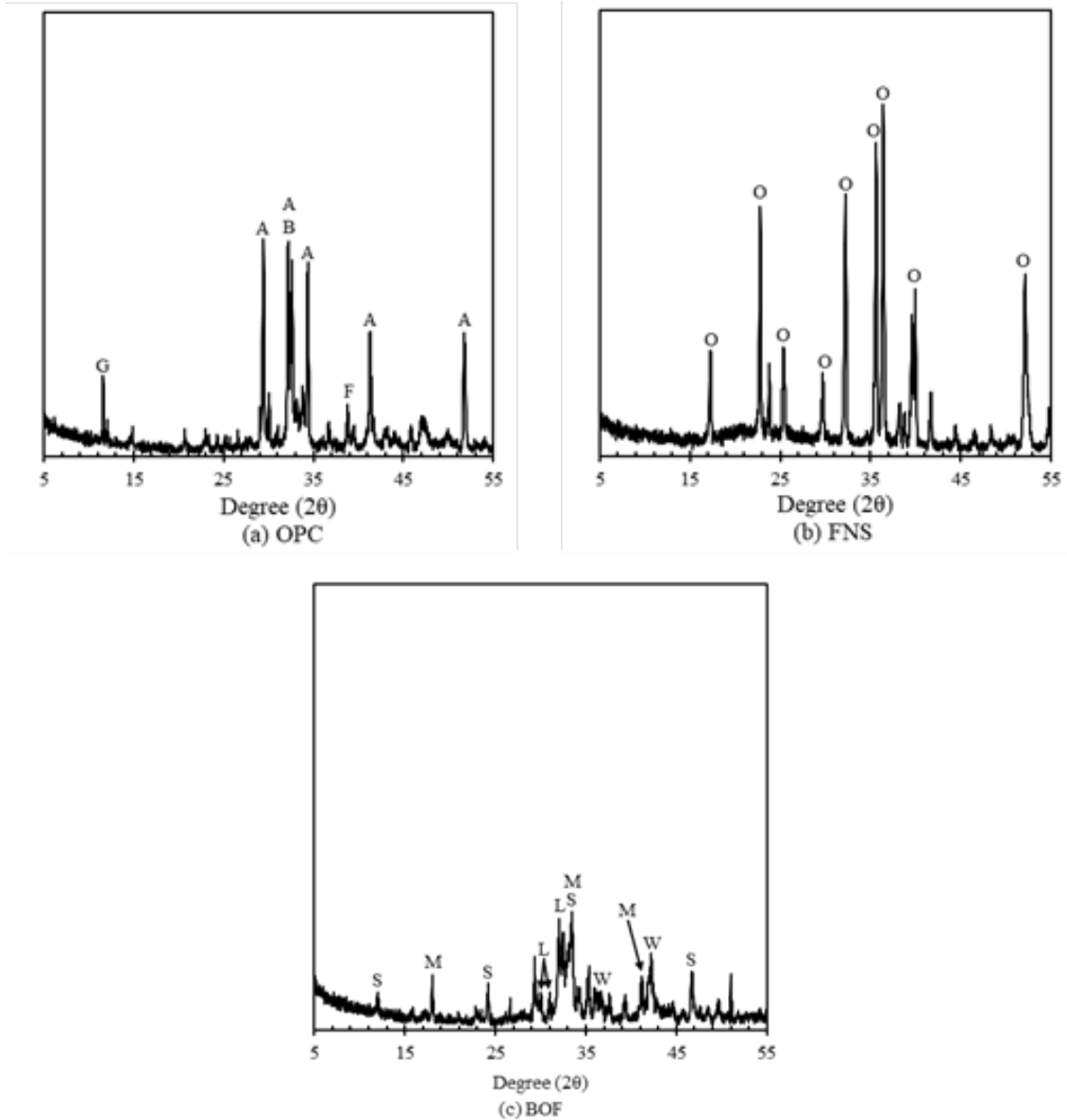
Figure 2: XRD curve of raw materials; (a) OPC, (b) FNS. A: Alite (C3S), B: Belite (C2S), F: Ferrite (C4AF), G: Gypsum (CaSO4), O: Olivine (Mg, Fe)2SiO4, W: Wuestite (FeO), S: Srebrodolskite (Ca2(Fe+3)2O5, M: Mayenite (Ca12Al14O33), L: Larnite (Ca2SiO4)

b) Mix proportion

The mix proportion of the specimen is shown in Table 2. The replacement ratio of 30% (by mass) FNS was chosen for the test specimen. For fine aggregates, washed aggregate with a specific gravity of 2.60 g/cm3 and fineness modulus of 2.73 was used. In the case of BOF fine aggregate, a specific gravity of 3.12 g/cm3 and a maximum size of 4.75 mm was employed.

To examine the hydration products, the mortar specimen was mixed with 0.45 of a total water-binder ratio (W/B). After mixing of the dry powder and fine aggregate with distilled water for 5 min., the mortar was placed into a cubic mold (50 × 50 × 50 mm), which was in turn cured at room conditions (20 ± 2 °C, RH 65 ± 5%) for 24 h. Then, the specimen was demolded and stored in a water bath (20 ± 2 °C) for specified periods. After it, the hardened mortar specimen was fragmented or ground off for its application to each microscopic examination, i.e. XRD analysis.

Table 2: Mix design of mortar (Kg/m3)

	OPC	FNS	BOF	Sand	Water
B20F30	381	163	267	1306	272

c) X-ray CT imaging

After curing for 90 days, the mortar specimens (50 × 50 × 50 mm) were kept in ambient temperature for 1 h stabilization of mass. Then, the sample was placed in CT scanning. The details of equipment and operation are given in Table 3 and the directional target was applied in this study. CT imaging process of mortar is suggested in Figure 3.

Table 3: X-ray Source

	Transmission Target	Directional Target	High Power Target
Voltage	30~120kV	30~225 kV	20~320kV
Forcal Spot size	0.4µm	6 µm	400 µm

For X-ray Detector specification is as below;
Type: Digital flat panel detector
Radiation energy: 40 ~ 320 kV
Active area: 400 mm (h) x 400 mm (v)
Pixel matrix: 1,024 (h) x 1,024 (v)
Pixel pitch: 200 µm
Resolution: 2.5 lp•mm@15 FPS(1×1), 1.25 lp•mm@30 FPS(2×2)

For X-ray Detector specification is as below;
Max. size of 3-D CT scanning: Ø 300 mm × 900 mm (h)
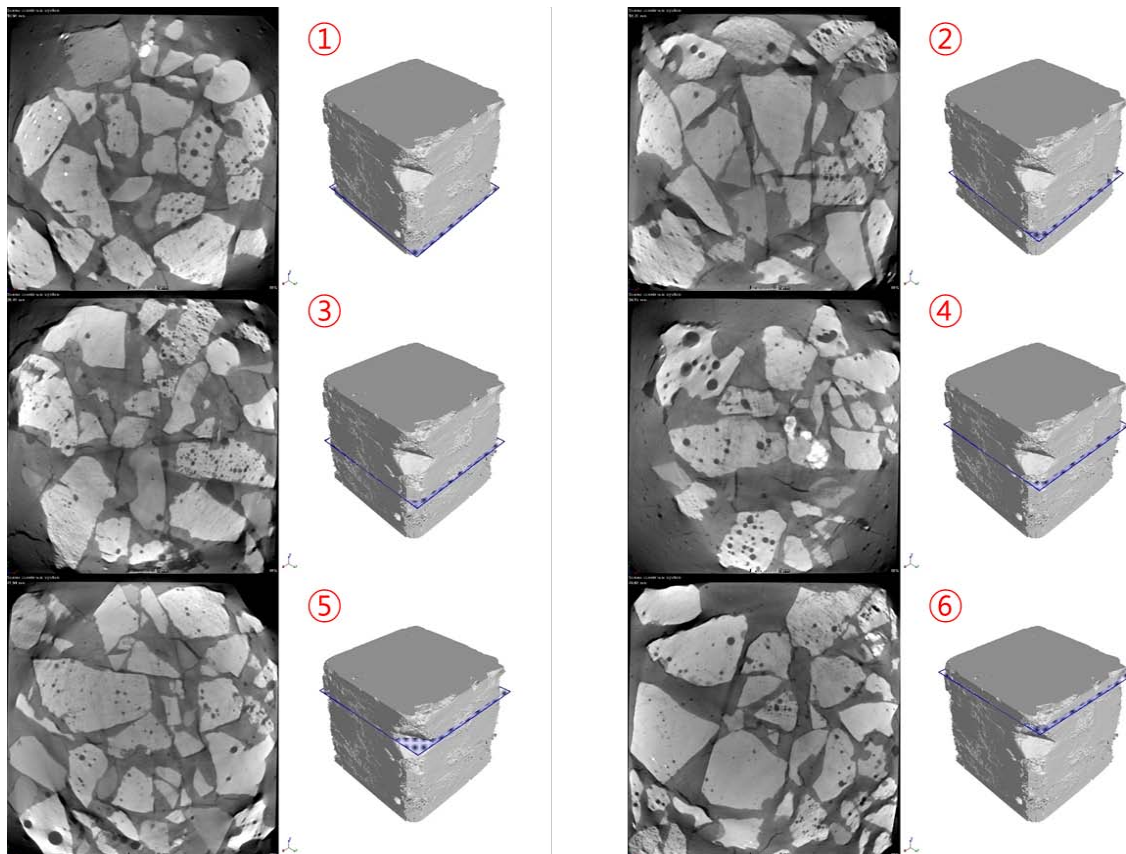Repetition accuracy: 0.004 °

Figure 3: CT scanning process of mortar

After scanning, the obtained images are filtered to remove the noises and segment the pores using OTSU (otsu algorithm) [17]. Then, reconstruct the obtained images into a 3D image in Avizo software [18]. Detailed scan conditions are described in Table 4.

Table 4: Scan condition [15]

Diameter (mm)	Voltage (kVp)	Current (mA)	Transmission Time (sec)	Source-Object Distance (mm)	Pixel Pitch (mm)
100	200	0.8	1	316	0.106488

III. Test Results

a) XRD test results

To figure out the hydraulic reactivity of B20F30 blended mortar containing OPC, FNS, and BOF fine aggregate, the XRD examination was performed for sieved mortars at 90 days, as given in Figure 4. Hydration products for B20F30 mainly include portlandite ($Ca(OH)_2$) and ettringite ($Ca_6Al_2(SO_4)_3$ $32H_2O$), calcite ($CaCO_3$), and anhydrate olivine crystalline ((Mg, $Fe)_2 \cdot SiO_4$), presumably being originated from raw FNS powder. These results indicated that FNS has low hydration reactivity. In fact, it is notable that there was no further formation of hydration products in B20F30 blended mortar. A formation of calcite may be attributed to the long-term curing age.
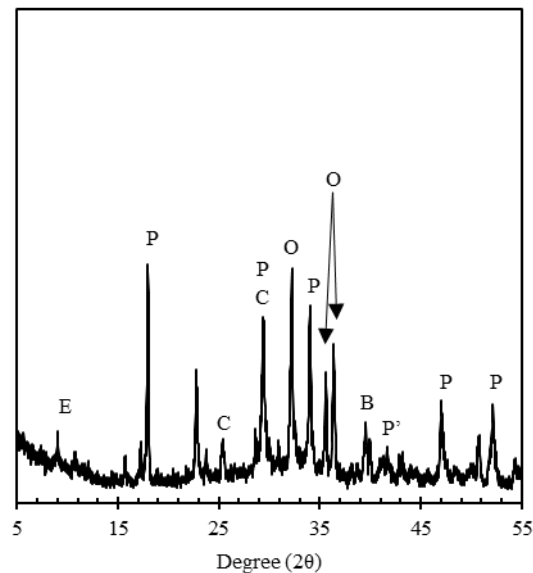

Figure 4: XRD curve of B20F30 mortar after 90 days of curing; E: Ettringite $Ca_6Al_2(OH)_{12}(SO_4)_3 26H_2O$, P: Portlandite ($Ca(OH)_2$), C: Calcite ($CaCO_3$), B: Brucite ($Mg(OH)_2$), P': Periclase ($MgO$), O: Olivine ($Mg$, $Fe)_2SiO_4$

b) X-ray Tomography

Figure 4 represents the 3D pore size distribution in mortar distinguished by red color. As shown in figure 4 (b), for B20F30 mortar, the average porosity was 2.268%. However, despite the low average porosity, large pores appearing dark red voids were detected in figure 4 (a), on the 3D image. In general, when performing the fraction in the 3D image process, voids were classified and indicated depending on their size and shape. For the case of dark red voids in figure 4 (a), those were seen as a BOF aggregate that was not excluded from the fractioning process due to physical characteristics of BOF which has an irregular shape.

As shown in Figure 4 (a) and (b), no expansion due to the incorporation of BOF aggregate was found. This may be ascribed to the reduction of cement clinker by FNS substitution. From the XRD test result in figure 2, free CaO which can contribute to the reaction of causing expansion was seen in figure 2 (a) OPC, whereas BOF in figure 2 (c) has consisted of crystalline phases except for Wustetite. Besides, it can be seen that the BOF aggregate has similar oxide composition as shown in table 1 and figure 2, which contributed to the hydration reaction in the cement matrix which cement clinker has been reduced due to the replacement by FNS incorporation. This is identical with the XRD test results in figure 3, both BOF aggregate clinker and new hydrates were not observed. Furthermore, the low reactivity of FNS was incorporated as seen in figure 4, B20F30 mortar shows a low porosity. This is because

low reactivity FNS contributed to the filler effect especially extra space; as the filler does not produce hydrates, at the same water to solids ratio, the water to clinker ratio is higher and there is more space for the hydration products of the clinker phases [19]. Thus, it can be said that there would be no adverse effect in using FNS and BOF aggregate for cementitious materials, presumably due to the no significant change of the hydration products and porosity.
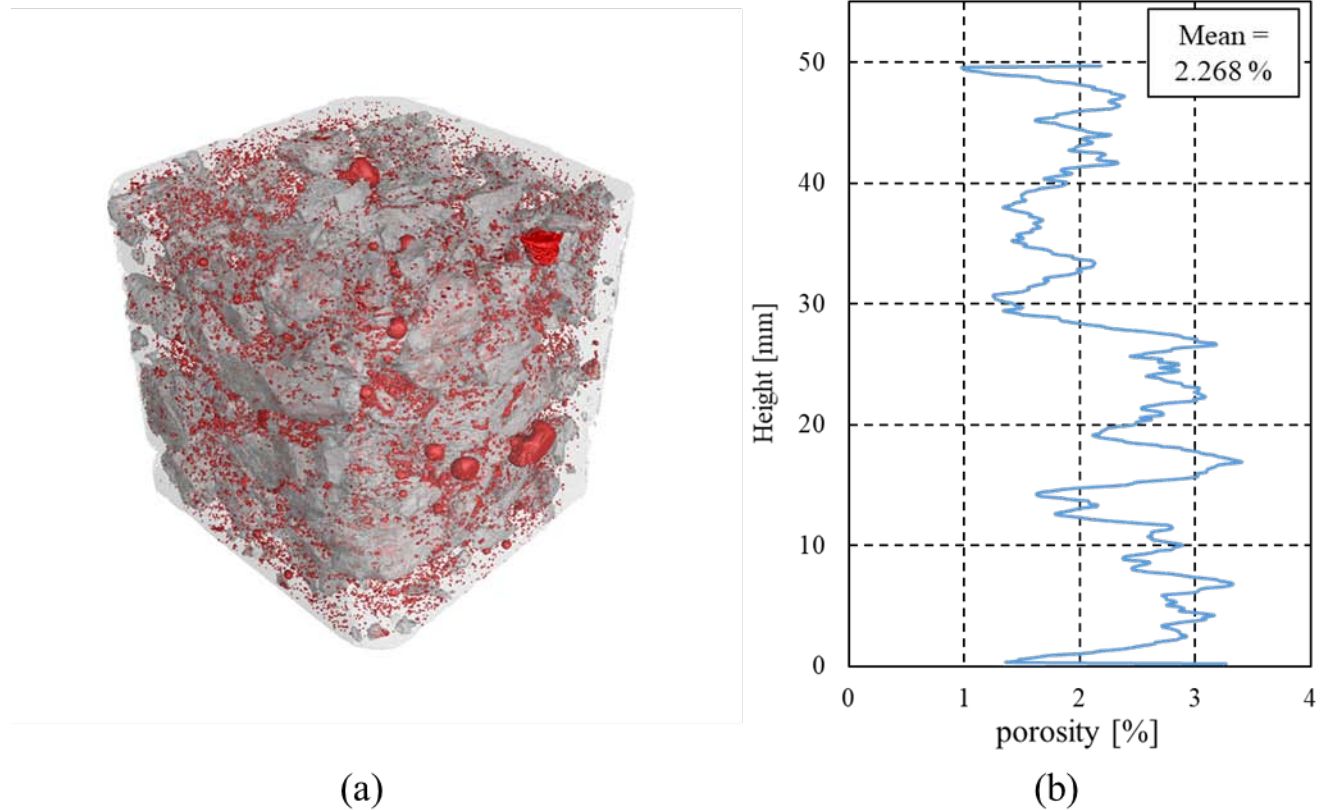

(a)

(b)

Figure 4: X-ray tomography of B20F30 mortar; (a) 3D image of mortar, (b) porosity with scan height

IV. Conclusion

In this study, the FNS cement with BOF fine aggregate mortar was investigated by the chemical microscopic analysis (X-ray fluorescence, X-ray diffraction) and pores distribution including an examination of X-ray CT analysis. Detailed experimental results and conclusion derived from the study are given as follows:

(1) The BOF aggregate has consisted of similar clinker of cement in XRD test results. For FNS, the composition mainly accounted for forsterite (Mg2SiO4) and fayalite (Fe2SiO4) which have crystalline nature. The low reactivity FNS contributed to the filler effect in the cement matrix while BOF aggregate clinker participated in the formation of hydration products. Moreover, there may be some reaction of BOF aggregate and cement matrix, due to similar clinker composition of BOF aggregate compared to OPC, there were no new hydrates found in B20F30 mortar.

(2) The apparent pore distribution and porosity were obtained by x-ray CT analysis at each height. The irregular shape of BOF aggregate resulted in large voids image in the 3D CT image. The large pores were detected in the 3D CT image while porosity with each height was 2.268%.

References Références Referencias

1. Sun, J., Feng, J., & Chen, Z. (2019). Effect of ferronickel slag as fine aggregate on properties of concrete. Construction and Building Materials, 206, 201-209.
2. Hiraskar, K. G., & Patil, C. (2013). Use of blast furnace slag aggregate in concrete. International Journal of Scientific & Engineering Research, 4(5), 95-98.
3. Das, B., Prakash, S., Reddy, P. S. R., & Misra, V. N. (2007). An overview of utilization of slag and sludge from steel industries. Resources, conservation and recycling, 50(1), 40-57.

4. Wang, K. X., Long, H. M., & Meng, Q. M. (2018). Steel slag cementitious activity and mechanism based on physical excitation. Iron Steel, 53(3), 82-86.

5. Zhao, J., Yan, P., & Wang, D. (2017). Research on mineral characteristics of converter steel slag and its comprehensive utilization of internal and external recycle. Journal of Cleaner Production, 156, 50-61.

6. Cho BS, Kim YU, Kim DB, Choi SJ (2018) Effect of ferronickel slag powder on microhydration heat, flow, compressive strength, and drying shrinkage of mortar. Advances in Civil Engineering 2018:1-7

7. Choi, Young Cheol, and Seongcheol Choi. "Alkali–silica reactivity of cementitious materials using ferro-nickel slag fine aggregates produced in different cooling conditions." Construction and Building Materials 99 (2015): 279-287.

8. Huang, Yiduo, Qiang Wang, and Mengxiao Shi. "Characteristics and reactivity of ferronickel slag powder." Construction and Building Materials 156 (2017): 773-789.

9. Sakoi, Yuki, et al. "Properties of concrete used in ferronickel slag aggregate." Proceedings of the 3rd international conference on sustainable construction materials and technologies, Tokyo, Japan. 2013.

10. KoNubu, K., and M. Shoya. "Guidelines for construction using Ferronickel slag fine aggregate concrete." Concrete library of JSCE 24 (1994).

11. Saha, Ashish Kumar, and Prabir Kumar Sarker. "Compressive strength of mortar containing ferronickel slag as replacement of natural sand." Procedia engineering 171 (2017): 689-694.

12. Saha, Ashish Kumar, and Prabir Kumar Sarker. "Expansion due to alkali-silica reaction of ferronickel slag fine aggregate in OPC and blended cement mortars." Construction and Building Materials 123 (2016): 135-142.

13. Lemonis, N., et al. "Hydration study of ternary blended cements containing ferronickel slag and natural pozzolan." Construction and Building Materials 81 (2015): 130-139.

14. Rahman MA, Sarker PK, Shaikh FUK, Saha AK (2017) Soundness and compressive strength of Portland cement blended with ground granulated ferronickel slag. Construction and Building Materials140:194-202.

15. Cho, W. J., Kim, M. J., & Kim, J. S. (2020). Study on the Pore Structure Characteristics of Ferronickel-Slag-Mixed Ternary-Blended Cement. Materials, 13(21), 4863.

16. Bernard, E.; Lothenbach, B.; Rentsch, D.; Pochard, I.; Dauzeres, A. Formation of magnesium silicate hydrates (M-S-H). Phys. Chem. Earth. 2017, 99, 142–157.

17. Vala, H.J.; Baxi, A. A review on Otsu image segmentation algorithm. Int. J. Adv. Res. Comput. Eng. Tehnol. (IJARCET) 2013, 2, 387–389.

18. Scientific, T.F. Amira-Avizo Software. Thermo Scientific™ Amira-Avizo Software (Oregon, USA) 2018.

19. Lothenbach, B., Scrivener, K., & Hooton, R. D. (2011). Supplementary cementitious materials. Cement and concrete research, 41(12), 1244-1256.